

# Detecting grain rotation at the nanoscale

Bin Chen<sup>a,b,c,1</sup>, Katie Lutker<sup>d</sup>, Jialin Lei<sup>e</sup>, Jinyuan Yan<sup>b,c</sup>, Shizhong Yang<sup>f</sup>, and Ho-kwang Mao<sup>a,g,1</sup>

<sup>a</sup>Center for High Pressure Science and Technology Advanced Research, Pudong, Shanghai 201203, China; <sup>b</sup>Advanced Light Source, Lawrence Berkeley National Laboratory, Berkeley, CA 94720; <sup>c</sup>Department of Earth and Planetary Sciences, University of California, Santa Cruz, CA 95064; <sup>d</sup>Department of Chemistry, University of California, Berkeley, CA 94720; <sup>e</sup>Department of Chemistry and Biochemistry, University of California, Los Angeles, CA 90095; <sup>f</sup>Department of Computer Science, Southern University, Baton Rouge, LA 70813; and <sup>g</sup>Geophysical Laboratory, Carnegie Institution of Washington, Washington, DC 20015

Contributed by Ho-kwang Mao, January 10, 2014 (sent for review December 10, 2013)

**It is well-believed that below a certain particle size, grain boundary-mediated plastic deformation (e.g., grain rotation, grain boundary sliding and diffusion) substitutes for conventional dislocation nucleation and motion as the dominant deformation mechanism. However, in situ probing of grain boundary processes of ultrafine nanocrystals during plastic deformation has not been feasible, precluding the direct exploration of the nanomechanics. Here we present the in situ texturing observation of bulk-sized platinum in a nickel pressure medium of various particle sizes from 500 nm down to 3 nm. Surprisingly, the texture strength of the same-sized platinum drops rapidly with decreasing grain size of the nickel medium, indicating that more active grain rotation occurs in the smaller nickel nanocrystals. Insight into these processes provides a better understanding of the plastic deformation of nanomaterials in a few-nanometer length scale.**

The plastic deformation of conventional polycrystalline metals has been well-studied. The plastic behavior of coarse-grained metals (with particle size larger than 100 nm) is mainly controlled by the nucleation and motion of lattice dislocations. Plastic deformation by dislocation glide results in crystallite rotations, generating lattice preferred orientation or texture. The anisotropic physical properties of a polycrystalline material are strongly related to the preferred alignment of its crystallites. Texture studies are of interest in many fields. In material science and engineering, texture control is essential in improving the strength and lifetime of structural materials (1). In Earth science, understanding texture development of minerals is important for interpreting seismic anisotropy in the Earth's interior (2–5).

The plastic deformation of nanomaterials has attracted much interest in recent years (6–12), but many controversies still exist (6–17). Various mechanisms have been reported (8, 11–18). It has been proposed that below a critical length scale the strength of nanometals would exhibit an inverse Hall-Petch size dependence because in the plastic deformation of fine nanocrystals, dislocation activity gives way to grain boundary (GB) sliding, diffusion, and grain rotation (7). If GB-mediated mechanisms dominate plastic deformation, it would yield a  $d^{-4}$  dependence on grain rotation rate, where  $d$  is the grain size (9), i.e., grain rotation activity would be greatly enhanced in fine nanocrystals. Grain-rotation-induced crystallographic alignment has been observed in 2–3-nm ferrihydrite nanocrystals (15–17). In contrast, computer simulations suggest that GB mobility drops with decreasing grain size (19, 20). Although the observation of grain rotation during deformation of micrometer-sized crystals is feasible (21, 22), in situ probing of grain rotation of ultrafine nanocrystals is difficult, precluding the direct exploration of mechanics at nanometer scales. Whether grain rotation becomes more active and dominant in finer nanocrystals is not yet experimentally verified. In this work, radial diamond-anvil cell (rDAC) X-ray diffraction (XRD) experiments (2) are used to make in situ observation of the texturing of stressed polycrystalline platinum in nickel media of various mean particle sizes, from 500 nm down to 3 nm.

The texturing change of platinum is expected to reflect some activity at the GBs of the nickel medium.

## Radial Diamond-Anvil Cell X-Ray Diffraction Measurements

We deformed the platinum and nickel mixture samples plastically in rDAs (Fig. S1). The nickel powders (Fig. S2) were pressed to form an ~10-μm-thick foil. Fragments of the foil were loaded in the gasket chamber. A small fragment of a few-micrometers-thick platinum foil was sandwiched by nickel foils. The XRD experiments were performed at beamline 12.2.2, Advanced Light Source, Lawrence Berkeley National Laboratory, Berkeley, CA. The platinum particles have a size of ~1 μm. The particle sizes of the nickel medium are  $500 \pm 45$  nm,  $20 \pm 8$  nm, and  $3 \pm 0.9$  nm, respectively. The relatively narrow size distributions allow the investigation of the size dependence of grain rotation. Both platinum and nickel particles are spherical in shape (Fig. 1). When shear stress is applied to polycrystals, individual crystals deform preferentially on slip planes. This results in crystal rotations that in turn lead to texture development (1). The radial diffraction images show variations in diffraction peak position with respect to the compression direction, indicating differential stresses in the material. They also display systematic intensity variations that can be used to deduce texture (Fig. 1 and Figs. S3–S6). For instance, the diffraction intensity of the platinum in 3-nm nickel at 37.0 GPa is minimal in the compression direction for the (111) diffraction peak, but it is maximal for the (220) peak (Fig. S5). The variations in diffraction intensity can best be seen in the “unrolled diffraction” images recorded as a function of diffraction angle (Fig. 2).

## Results and Discussion

Rietveld refinement with MAUD software was used to analyze the differential stress (23), microstructure, and texture of the

### Significance

**The plastic deformation of nanomaterials has long been wrapped in mystery. Grain rotation is suggested to be a dominant mechanism of plastic deformation for ultrafine nanomaterials. However, the in situ observation of grain rotation has been made possible only for coarse-grained materials. Here we report the in situ high-pressure detection of grain rotation at the nanoscale. The surprising observation is that the texture strength of the same-sized platinum drops rapidly with decreasing grain size of the nickel medium, indicating that more active grain rotation occurs in the smaller nickel nanocrystals. Insight into these processes provides a better understanding of the plastic deformation of nanomaterials at a few-nanometer length scale.**

Author contributions: B.C. and H.-k.M. designed research; B.C., K.L., J.L., J.Y., and S.Y. performed research; B.C. analyzed data; and B.C. wrote the paper.

The authors declare no conflict of interest.

Freely available online through the PNAS open access option.

<sup>1</sup>To whom correspondence may be addressed. E-mail: chenbin@hpstar.ac.cn or hmao@ciw.edu.

This article contains supporting information online at [www.pnas.org/lookup/suppl/doi:10.1073/pnas.1324184111/-DCSupplemental](http://www.pnas.org/lookup/suppl/doi:10.1073/pnas.1324184111/-DCSupplemental).

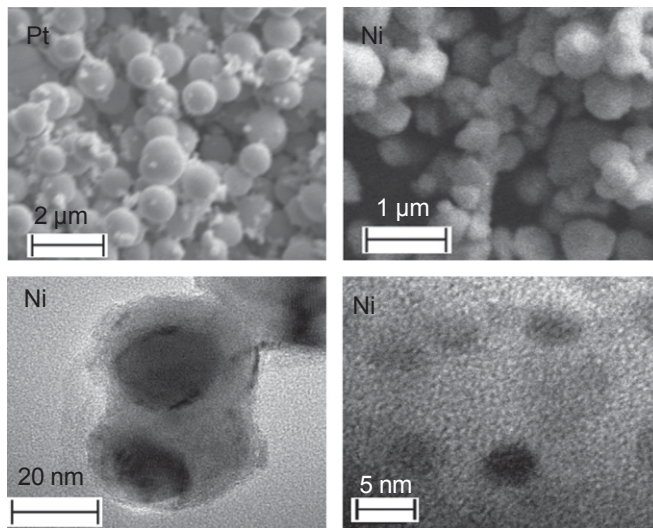


**Fig. 1.** Scanning electron microscopy (SEM) images of bulk-sized platinum (*Upper Left*) and nickel (*Upper Right*) before compression, and transmission electron microscopy (TEM) images of the 20 (*Lower Left*) and 3 nm (*Lower Right*) nickel particles as synthesized.

samples at each pressure. Texture is represented with inverse pole figures (IPFs) of the compression direction (Fig. 3 and Fig. S7). These show the probability of finding the poles (normal) to lattice planes in the compression direction. The IPF maximum of coarse nickel particles is at the (110) corner (Fig. S7), indicating that the (110) lattice planes are oriented at high angles to the compression direction, consistent with  $\{111\} <110>$  slip of fcc crystals. As shown in Fig. 4, at 35 GPa the intensity maxima positions of diffraction line (111) of platinum and 500-nm nickel differ by about  $17^\circ$  in term of azimuthal angle. Accordingly, the IPF maximum of platinum does

not appear around the (110) corner, different from the typical IPF profile of fcc crystals under uniaxial compression, suggesting that the strain heterogeneity occurs in platinum. This may arise from the low content of platinum in the sample mixture. The loaded platinum sample is very thin. The low diffraction intensity of platinum relative to nickel media indicates the low platinum content. Therefore, the shear mode in platinum, more like a plane strain mode, is different from the compressional shear mode in the nickel media. This is evident by the asymmetric profile of the diffraction ring of Pt (111) about the compression axis (vertical) (Fig. 4).

A surprising observation is that the texture strength of platinum drops systematically with decreasing particle size of the nickel media (Fig. 3). The changes in the texture strength of nickel media reflect the change of dislocation- and GB-mediated activities in different-sized nickel nanocrystals (Fig. S7). However, the particle sizes of the platinum sample in all runs are the same. At the same stress level, the texturing of the same-sized platinum should be closely similar if the GB interaction between platinum and nickel particles is the same. As shown in Fig. 3, obvious change in texturing strength is observed in platinum. For instance, at around 37 GPa, the texture strength of platinum is 2.7 and 1.5 multiples of random distribution (m.r.d.) in 500- and 20-nm nickel medium, respectively. It drops to 1.2 m.r.d. in 3-nm nickel medium. The large texture loss of platinum can arise from two factors: (*i*) the lack of shear stress due to the loss of pressure gradients, or (*ii*) the enhanced grain rotation in fine nanocrystals that destroys the texture of neighboring platinum particles.

From the differential strain of lattice, differential stress and thus shear stress can be calculated. According to the MAUD analysis, at  $\sim 37$  GPa the shear stress in platinum with 3-, 20-, and 500-nm nickel medium is about 2.2, 1.9, and 1.5 GPa, respectively (Table 1). According to dislocation theory (8, 26), with the approximation that the source size is equal to the particle size ( $D$ ), the critical shear stress needed to nucleate a full dislocation is

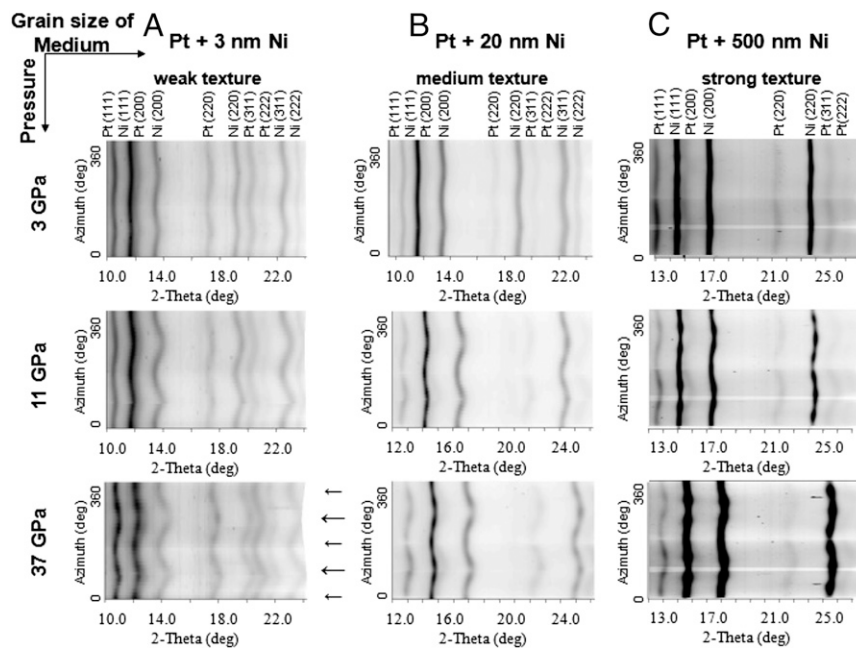


**Fig. 2.** Azimuthally ( $0\text{--}360^\circ$ ) unrolled diffraction images of 1-μm platinum in 3-nm (*A*), 20-nm (*B*), and 500-nm (*C*) nickel media. To enable direct comparison between runs, pressures are rounded (precise values are given in Fig. 3). The long black arrows represent the maximal compression direction and the short arrows the minimal compression direction. The curvature within the diffraction lines indicates that the sample is stressed. Texture is evident as the systematic intensity variations of the diffraction peaks along the azimuthal direction. The diffraction of platinum mixed with 20- and 3-nm nickel particles at 3 GPa was taken with an X-ray wavelength of  $0.4133 \text{ \AA}$ . For all other measurements, a wavelength of  $0.4959 \text{ \AA}$  was used.

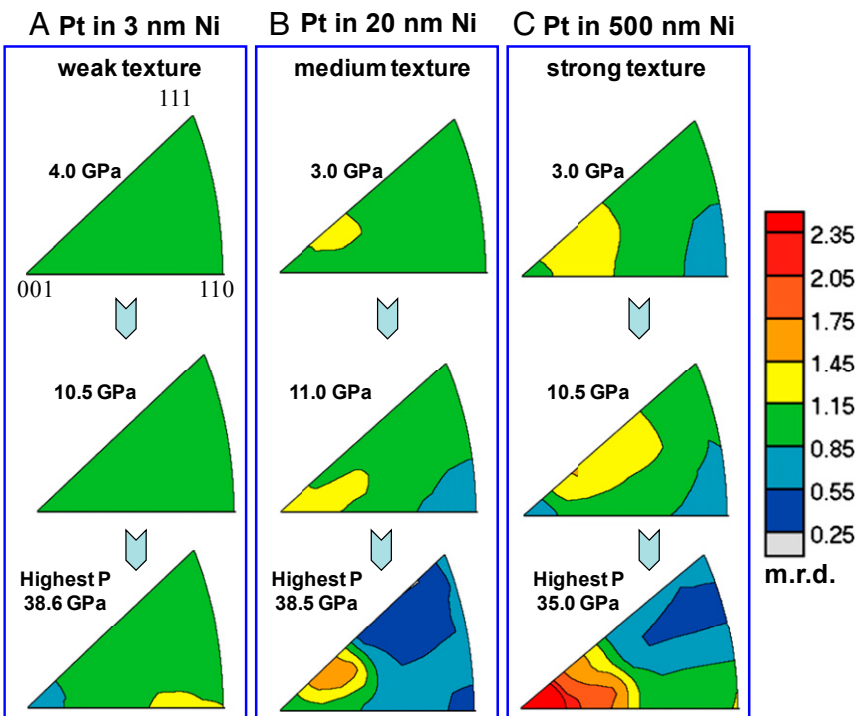


**Fig. 3.** Inverse pole figures of platinum in 3-nm (*A*), 20-nm (*B*), and 500-nm (*C*) nickel media along the compression direction (normal direction). Equal area projection and a linear scale are used. (The texture scale is renormalized in BEARTEX for replotted under the same color scale.) The degree of lattice preferred orientation (texture strength) is expressed as multiples of random distribution (m.r.d.), where m.r.d. = 1 denotes random distribution and a higher m.r.d. number represents stronger texture. The inverse pole figures of the nickel media are shown in Fig. S7.

$$\tau_f = \frac{2aGb_f}{D}, \quad [1]$$

where  $b_f$  is the Burgers vector, and  $G$  is the shear modulus. The factor  $a$  is taken to be 0.5 for edge dislocations and 1.5 for screw dislocations. It is estimated that the critical shear stress for nucleation of an edge dislocation in 1-μm platinum is 0.1 GPa. The measured shear stress is far above this value. Dislocations can form in the platinum in all cases with the three nickel media, which is confirmed with the texturing of platinum in 500-nm nickel. As shown in Fig. 2, the large curvatures of the 2D diffraction lines of nickel nanocrystals also provide strong evidence for the shear stress in ultrafine nickel nanocrystals (24, 27). Therefore, it is excluded that the observed texture loss of platinum in ultrafine nickel media arises from the lack of shear stress. The grain rotation of nickel media is likely to account for the texture loss.

It is known that dislocation glide on preferred slip systems gives rise to crystallographic texture whereas grain rotation or GB sliding alone randomizes the grain orientation distribution

(6, 28). It is found that grain rotation is driven by the change of GB energy (28). The angle between boundaries is a measure of the relative energies of the GBs. Deformation-induced grain shape changes, GB diffusions, nucleation, and motion of dislocations usually lead to the change of GB angles, and grains rotate to minimize interfacial energies. Previous observations indicate that grain rotation is random. Therefore, the textures, in favor of the operative slip systems, can be destroyed by GB-mediated grain rotation.

Uniaxial compression provides the shear stress that generates dislocation nucleation, and fiber textures hence form in the platinum. The texture is reasonably strong in platinum mixed with 500-nm nickel. An obvious drop of texture strength can be seen when mixed with 20-nm nickel medium. Surprisingly, the textures of the same bulk-sized platinum get almost completely lost when mixed with 3-nm nickel medium. The systematic texture loss of the platinum provides compelling evidence that deformation-induced grain rotation is strongly grain size dependent.

The physics behind the observed texture loss due to the nickel media can be understood by considering the size and pressure

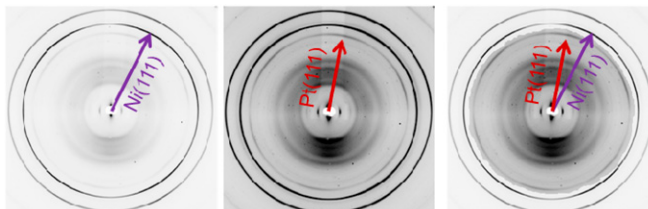


**Fig. 4.** At 35 GPa, the intensity maxima of diffraction line (111) of platinum and 500-nm nickel differ greatly in position. (*Left*) The two plots are the same diffraction image with different intensity contrast for better view of Ni (111) and Pt(111), respectively. (*Right*) Overlapping of the left two images for comparing the position of diffraction intensity maxima.

**Table 1. Differential stress of platinum mixed with nickel medium**

Pressure, GPa	In 500 nm Ni, GPa	In 20 nm Ni, GPa	In 3 nm Ni, GPa
3	0.4	1.9	1.8
11	2.7	2.8	2.4
37	3.0	3.8	4.3

The differential stress obtained from the fit to the experimental data provides an estimate of shear stress as well as a lower-bound estimate of materials' shear strength (24). The elastic constants of platinum at pressure used for the data fit are from ref. 25.

**Table 2.** Calculated critical shear stress needed for nucleation of dislocations (Eq. 1)

Particle size of nickel	3 nm		20 nm		500 nm	
Type of dislocations	Edge, GPa	Screw, GPa	Edge, GPa	Screw, GPa	Edge, GPa	Screw, GPa
Critical shear stress for nucleation of a full dislocation (theoretical)	12.3	37.0	1.8	5.4	0.1	0.2

For the calculations,  $b_p = 0.244$  nm (9),  $G = 76$  GPa (27, 29),  $\nu = 0.31$  (27).

effects on the dislocations. As shown in Table 2, the critical shear stress for dislocation nucleation increases dramatically with decreasing particle size. At the same stress level, generation of dislocations is relatively easier in coarser crystals. At pressure, compression-induced deformation leads to energy increase of the samples. Dislocation content is larger in coarse crystals. The motion of dislocations results in plastic deformation and grain shape change to minimize the system energy and equilibrate the interactions among neighboring grains. Coarse grains need larger torque and energy for rotation and hence have a low rotation rate (28). In finer nanocrystals, much higher shear stress is needed for the nucleation of dislocations. Dislocations play little part in equilibrating the system. Instead, grains rotate to minimize the compression-induced energy increase. Therefore, finer nanocrystals have a higher rotation rate (28). The grain rotation of nickel nanocrystals leads to rotation of neighboring platinum particles. The orientations of platinum particles are hence changed, which results in the loss of texture.

These results emphasize the importance of rDSC XRD experimentation in assessing plastic deformation in nanomaterials. Through a combination of textural and stress analysis, the size effect on grain rotation can be assessed. Our results demonstrate

that grain rotation is much more active in finer nanocrystals. Such *in situ* high-pressure textural studies thus provide the means to investigate deformation mechanisms and help constrain the fundamental physics of deformation at the nanoscale.

**ACKNOWLEDGMENTS.** B.C. and K.L. thank A. P. Alivisatos for discussion. B.C. thanks Warunporn Kanitpanyacharoen, Hans-Rudolf Wenk, Selva Vennila Raju, Jason Knight, Alastair MacDowell, and Quentin Williams for technical help and discussion. The X-ray diffraction measurements were made at Beamlines 12.2.2 and 12.3.2 of the Advanced Light Source, Lawrence Berkeley National Laboratory. Some test measurements were made at BL15U1 of the Shanghai Synchrotron Radiation Facility, China. Financial support for this work was provided by National Science Foundation (NSF), including from the Consortium for Materials Properties Research in Earth Sciences under NSF Cooperative Agreement EAR 10-43050. The Advanced Light Source is supported by the Director, Office of Science, Office of Basic Energy Sciences, of the US Department of Energy (DOE) under Contract DE-AC02-05CH11231. J.L. and S.Y. are supported by NSF-Louisiana Alliance for Simulation-Guided Materials Applications program (EPS-1003897); National Aeronautics and Space Administration/Louisiana Education Quality Support Fund (2009-2012)-Phase3-03; DOE Awards DE-FE0007220, DE-FE0011550, DE-FE0008382, and DE-FE0004734; and the Department of Computer Science. K.L. is supported by the Physical Chemistry of Semiconductor Nanocrystals Program, KC3105, Office of Basic Energy Science of the US DOE under Contract DE-AC02-05CH11231. H.-K.M. was supported as part of Energy Frontier Research in Extreme Environments Center, an Energy Frontier Research Center funded by the US DOE, Office of Science, Office of Basic Energy Sciences under Award DE-SG0001057.

- Kocks UF, Tome ÁCN, Wenk H-R (2000) in *Texture and Anisotropy, Preferred Orientations in Polycrystals and Their Effect on Materials Properties* (Cambridge Univ Press, Cambridge, UK), 2nd ed., p. 676.
- Miyagi L, Kanitpanyacharoen W, Kærcher P, Lee KKM, Wenk H-R (2010) Slip systems in MgSiO<sub>3</sub> post-perovskite: Implications for D'' anisotropy. *Science* 329(5999): 1639–1641.
- Merkel S, et al. (2006) Plastic deformation of MgGeO<sub>3</sub> post-perovskite at lower mantle pressures. *Science* 311(5761):644–646.
- Li B, Liebermann RC (2007) Indoor seismology by probing the Earth's interior by using sound velocity measurements at high pressures and temperatures. *Proc Nat Acad Sci USA* 104(22):9145–9150.
- Selim FA, et al. (2013) Positron lifetime measurements of hydrogen passivation of cation vacancies in yttrium aluminum oxide garnets. *Phys Rev B* 88(17):4102.
- Weissmüller J, Markmann J (2005) Deforming nanocrystalline metals: New insights, new puzzles. *Adv Eng Mater* 7(4):202–207.
- Schiottz J, Jacobsen KV (2003) A maximum in the strength of nanocrystalline copper. *Science* 301(5638):1357–1359.
- Chen MW, et al. (2003) Deformation twinning in nanocrystalline aluminum. *Science* 300(5623):1275–1277.
- Shan Z, et al. (2004) Grain boundary-mediated plasticity in nanocrystalline nickel. *Science* 305(5684):654–657.
- Budrovic Z, Van Swygenhoven H, Derlet PM, Van Petegem S, Schmitt B (2004) Plastic deformation with reversible peak broadening in nanocrystalline nickel. *Science* 304(5668):273–276.
- Lu L, Chen X, Huang X, Lu K (2009) Revealing the maximum strength in nanotwinned copper. *Science* 323(5914):607–610.
- Li X, Wei Y, Lu L, Lu K, Gao H (2010) Dislocation nucleation governed softening and maximum strength in nano-twinned metals. *Nature* 464(7290):877–880.
- Yamakov V, Wolf D, Phillpot SR, Mukherjee AK, Gleiter H (2002) Dislocation processes in the deformation of nanocrystalline aluminium by molecular-dynamics simulation. *Nat Mater* 1(1):45–48.
- Kumar KS, Suresh S, Chisholm MF, Horton JA, Wang P (2003) Deformation of electrodeposited nanocrystalline nickel. *Acta Mater* 51(2):387–405.
- Banfield JF, Welch SA, Zhang H, Ebert TT, Penn RL (2000) Aggregation-based crystal growth and microstructure development in natural iron oxyhydroxide biomimetic products. *Science* 289(5480):751–754.
- Alivisatos AP (2000) Biomimetic mineralization. Naturally aligned nanocrystals. *Science* 289(5480):736–737.
- Murayama M, Howe JM, Hidaka H, Takaki S (2002) Atomic-level observation of dislocation dipoles in mechanically milled, nanocrystalline Fe. *Science* 295(5564): 2433–2435.
- Penn RL, Banfield JF (1998) Imperfect oriented attachment: Dislocation generation in defect-free nanocrystals. *Science* 281(5379):969–971.
- Farkas D, Mohanty S, Monk J (2007) Linear grain growth kinetics and rotation in nanocrystalline Ni. *Phys Rev Lett* 98(16):165502–165505.
- Gutkin MY, Ovid'ko IA (2005) Grain boundary migration as rotational deformation mode in nanocrystalline materials. *Appl Phys Lett* 87(25):251916.
- Margulies L, Winther G, Poulsen HF (2001) In situ measurement of grain rotation during deformation of polycrystals. *Science* 291(5512):2392–2394.
- Jakobsen B, et al. (2006) Formation and subdivision of deformation structures during plastic deformation. *Science* 312(5775):889–892.
- Lutterotti L, Matthies S, Wenk H, Schultz AS, Richardson JW (1997) Combined texture and structure analysis of deformed limestone from time-of-flight neutron diffraction spectra. *J Appl Phys* 81(2):594–600.
- Chung H-Y, et al. (2007) Synthesis of ultra-incompressible superhard rhenium diboride at ambient pressure. *Science* 316(5823):436–439.
- Menéndez-Proupin E, Singh AK (2007) Ab initio calculations of elastic properties of compressed Pt. *Phys Rev B* 76(5):054117.
- Hirth JP, Lothe J (1992) *Theory of Dislocations* (Krieger Publishing Company, Malabar, FL), 2nd Ed.
- Chen B, et al. (2012) Texture of nanocrystalline nickel: Probing the lower size limit of dislocation activity. *Science* 338(6113):1448–1451.
- Harris KE, Singh VV, King AH (1998) Grain rotation in thin films of gold. *Acta Mater* 46(8):2623–2633.
- Çain T, Pettitt BM (1989) Elastic constants of nickel: Variations with respect to temperature and pressure. *Phys Rev B Condens Matter* 39(17):12484–12491.